ORNL/TM-2023/2978

Start-up Operation Experience with a Liquid Fluoride Salt Forced Convection Loop

Graydon Yoder, Jr.
Kevin R. Robb
Elvis Dominguez-Ontiveros
David K. Felde
David L. Fugate
David E. Holcomb

August 2023

OAK RIDGE National Laboratory

ORNL IS MANAGED BY UT-BATTELLE LLC FOR THE US DEPARTMENT OF ENERGY

DOCUMENT AVAILABILITY

Reports produced after January 1, 1996, are generally available free via OSTI.GOV.

Website www.osti.gov

Reports produced before January 1, 1996, may be purchased by members of the public from the following source:

National Technical Information Service
5285 Port Royal Road
Springfield, VA 22161
Telephone 703-605-6000 (1-800-553-6847)
TDD 703-487-4639
Fax 703-605-6900
E-mail info@ntis.gov
Website http://classic.ntis.gov/

Reports are available to US Department of Energy (DOE) employees, DOE contractors, Energy Technology Data Exchange representatives, and International Nuclear Information System representatives from the following source:

Office of Scientific and Technical Information
PO Box 62
Oak Ridge, TN 37831
Telephone 865-576-8401
Fax 865-576-5728
E-mail reports@osti.gov
Website https://www.osti.gov/

ORNL/TM-2023/2978

Nuclear Energy and Fuel Cycle Division

START-UP OPERATION EXPERIENCE WITH A LIQUID FLUORIDE SALT FORCED CONVECTION LOOP

Graydon Yoder, Jr.
Kevin R Robb
Elvis Dominguez-Ontiveros
David K Felde
David L Fugate
David E Holcomb

August 2023

Prepared by
OAK RIDGE NATIONAL LABORATORY
Oak Ridge, TN 37831
managed by
UT-BATTELLE LLC
for the
US DEPARTMENT OF ENERGY
under contract DE-AC05-00OR22725

CONTENTS

LIST OF FIGURES

LIST OF TABLES

ABBREVIATIONS

AHTR	advanced high temperature reactor
ANP	Aircraft Nuclear Propulsion
FHR	fluoride salt cooled high temperature reactor
LSTL	liquid salt test loop
MCRE	Molten Chloride Reactor Experiment
MSBR	the molten salt breeder reactor
MSFR	molten salt fast reactor
MSR	molten salt reactor
MSRE	Molten Salt Reactor Experiment
ORNL	Oak Ridge National Laboratory
PB-AHTR	pebble bed–AHTR
RMS	root mean square
SiC	silicon carbide
SmAHTR	small fluoride salt-cooled high temperature reactor

ACKNOWLEDGEMENTS

This material is based upon work supported by the US Department of Energy Office of Nuclear Energy and the Shanghai Institute of Applied Physics through a Cooperative Research and Development Agreement.

FOREWORD ON REPORT CONTEXT

This report was developed in early 2017 after the successful initial operation of the forced flow salt loop in 2016. The report was not published at that time because of staff retirements and a temporary pause in the project. The report was revisited and was deemed to provide valid technical insights not published elsewhere, as well as historical context on the re-establishment of molten halide salt research in the United States. Therefore, this report has been released without modifying the content from the 2017 version except for minor editorial revisions. Additional commentary has been added as footnotes in the "Introduction" and "Background" sections to provide current context to some statements.

ABSTRACT

A liquid fluoride salt forced convection test loop was constructed at Oak Ridge National Laboratory. Its unique features include a pebble bed test section, high-temperature instrumentation, a noncontact rotating gas seal for the pump, a silicon carbide flow tube, and a unique inductive heating technique. Initial start-up and shake-down testing has been completed. This paper describes how several of the systems performed, highlights those that worked well, and discusses issues that arose during the start-up process. This discussion should be of interest to those who intend to develop molten salt technologies and who are interested in some of the specific techniques used in this experiment.

1. INTRODUCTION

At high temperatures, liquid fluoride salts have thermophysical properties (i.e., volumetric heat capacity, thermal conductivity, and viscosity) similar to water. Because of their high boiling point, fluoride salts can be used to design single-phase heat transport systems at temperatures well above those that use water as a heat transfer medium. Renewed interest in fluoride salts includes their use in solar energy systems, fusion energy blanket devices, and advanced fission reactor designs. The latter is the focus of the facility discussed in this paper.

Multiple advanced fission reactor design concepts have been proposed. These concepts include fluoride salt–cooled reactor designs, as well as fluoride salt–fueled reactor designs. Both design concepts will require extensive development efforts before commercial versions can be realized. Although substantial efforts were made to develop fluoride salt coolant during the 1960s and 1970s, more recently this technology has been relatively dormant.[a]New experimental facilities and test equipment are needed to extend and enhance the technology and to recapture the practical knowledge developed through experience.

The liquid salt test loop (LSTL) at Oak Ridge National Laboratory (ORNL) was developed not only to recapture some of the previous experience, but also to incorporate new technology that has been developed in the intervening years. Several accomplishments have been achieved during the development and operation of the LSTL. These include the use of silicon carbide (SiC) as a piping material, development of sealing and gasketing techniques to connect SiC to metal piping systems, incorporation of a noncontact gas rotating seal as part of the liquid salt pump, high–temperature instrumentation, and an inductive heating system that simulates prototypic volumetric heating of nuclear reactor fuel. The LSTL is the first forced convection high-temperature fluoride salt system to operate in the United States in approximately 40 years.

Several observations were noted during the loop's start-up and shakedown processes, and issues were identified and analyzed that should help those developing fluoride salt–based experiments. The discussion that follows highlights several operational features and problems that were encountered during LSTL start-up.

[a] Context content: Over the last several years, efforts to develop molten halide salts have expanded significantly. As noted in the "Background" section, multiple companies are currently pursuing development of molten salt reactor concepts. In addition, R&D efforts have expanded at universities and national laboratories.

2. BACKGROUND

Major interest in the fluoride salts as a heat transfer medium started during the Aircraft Nuclear Propulsion (ANP) program in the late 1940s. A high-temperature heat transfer medium was needed to develop a lightweight nuclear power source that could be used to support long duration aircraft flights. The initial design of the aircraft nuclear reactor used a liquid sodium coolant combined with a solid fuel. However, because of reactor physics issues with this design, as well as structural concerns over the solid fuel, the project eventually turned to the use of a liquid fuel consisting of sodium, zirconium, and uranium fluoride salts. The ANP program continued for approximately 12 years and included operation of the first molten salt reactor (MSR), the Aircraft Reactor Experiment, at ORNL.[1–4] This reactor operated for 9 days in 1954 at a steady outlet temperature of 850°C and at powers up to 2.5 MW. Although the ANP program officially ended in 1961, ANP program researchers realized early on that liquid salt–fueled reactors could serve as commercial power reactors given the attractive characteristics of the fluoride salts.

Investigation into the application of MSRs for civilian power started in the late 1950s. In 1960, the design of a new molten salt–fueled experimental reactor, the Molten Salt Reactor Experiment (MSRE), was initiated at ORNL to support development of the commercial version of this reactor. MSRE was fueled with a mixture of uranium, lithium, beryllium, and zirconium fluorides. It was constructed of INOR-8 (now Hastelloy-N), a material developed specifically for molten salt application. Using much of the infrastructure that was developed for the ARE, the MSRE went critical in 1965 and operated for approximately 4 years. During one period, the reactor operated for 6 months continuously at powers up to ~8 MW. This testing demonstrated that the reactor could be operated stably and that its components were reliable. MSRE was also the first reactor ever to operate fueled with ^{233}U. Haubenreich and Engle provide a good summary of the MSRE test program.[5]

The MSR program continued into the early 1970s and was primarily focused on developing the molten salt breeder reactor (MSBR) concept,[6] developing full-scale reactor designs, and evaluating the economics of these systems. The MSBR program was discontinued in 1974 in favor of the sodium fast breeder reactor design, and work on MSRs essentially stopped for several decades as funding was focused on the sodium fast breeder reactor design.

The ANP, MSRE, and MSBR programs produced much of the existing data on fluoride salts and fluoride salt reactors. A significant amount of the research performed within these programs covered areas such as materials compatibility with the salts,[7] salt physical properties,[8–10] heat transfer characteristics,[11] neutronics behavior,[12] component development,[13] salt purification and handling techniques,[14] and salt eutectic characterization.[15] Hundreds of papers and reports were generated during the course of these programs. The references here are only a few examples, but they provide an entrance point into this literature. A partial list with links to ORNL reports on the subject can be found in the resource compiled by Hogland.[16]

After a long hiatus, interest was renewed in fluoride salts as a reactor fuel and coolant in 2002, when the Generation IV reactor program[17, 18] selected the molten salt concept as one of the 6 reactor types to be investigated. A molten salt design was included in the down-select because when they are used as a coolant, liquid salts allow high-temperature operation at relatively low pressures compared to water- and gas-cooled reactor designs. Liquid salts also have excellent heat transfer characteristics when compared to gas systems, and unlike liquid metal systems, they are inert.

Initially, the molten salt portion of the program focused on traditional liquid salt–fueled models using uranium or thorium fuel. However, shortly after the Generation IV program began, a second concept emerged that used fluoride salt as coolant but combined it with a solid fuel.[19] This configuration is called the *advanced high temperature reactor* (AHTR) or the *fluoride salt cooled high temperature reactor*

(FHR). Other Generation IV concepts—for instance some configurations of the very high-temperature reactor, a gas-cooled concept—also use liquid salts as the heat transfer medium in the intermediate cooling loop because of their attractive heat transfer properties.

Within the Generation IV International Forum, France and Euratom[b] have been working on the liquid salt–fueled reactor concept, focusing on a molten salt fast reactor (MSFR) design.[20, 21] The International Atomic Energy Agency recently announced the initiation of a new platform for MSR technical collaboration.[22] The FHR design is primarily being pursued in the United States by ORNL,[23–25] which is developing several FHR concepts, and by a university consortium led by the Massachusetts Institute of Technology, the University of California, Berkeley, and the University of Wisconsin,[26, 27] which are developing a concept using solid fuel imbedded in graphite pebbles—the pebble bed–AHTR (PB-AHTR). A second university consortium led by the Georgia Institute of Technology, which includes Ohio State University, Texas A&M University, AREVA, and ORNL, is developing analysis techniques, specific technologies (e.g., high-temperature instrumentation, materials corrosion behavior), and licensing strategies.[28]

China[b] has a very active liquid salt reactor development program,[29] with multiple experimental efforts designed to culminate in a test reactor using a pebble bed fuel design. China is also developing a molten salt–fueled reactor design building on information gathered from the pebble bed test reactor. The European Union is currently sponsoring the Safety Assessment of the Molten Salt Fast Reactor project to evaluate the safety aspects of fast spectrum MSRs.[30] The Czech Republic is involved in fluoride salt experimentation[31] and has performed neutronics testing using FLiBe salt that was originally used in MSRE (FLiBe is a eutectic consisting of 67% LiF and 33% BeF_2). India is developing an FHR concept called the *Innovative High Temperature Reactor*[32] that uses a pebble bed core design. The Soviet Union also initiated a significant effort during the 1970s which continues into the present as led by the Kurchatov Institute to study a variety of aspects of molten salt coolant. They have conducted several reactor design and optimization studies and has performed materials development and implemented compatibility testing programs.[33, 34]

Several recently formed small companies[c] are proponents of the MSR concept, including TerraPower,[35] Terrestrial Energy,[36] Flibe Energy,[37] Transatomic Power,[38] Elysium Industries,[39] and ThorCon.[40] Some of these companies promote specific MSR concepts, whereas others promote the concept in general or focus on specific MSR aspects. The US government recently reinitiated MSR support by funding industry-led efforts to develop MSR technologies.[41, 42]

Even during the early years as MSRs were first being developed, fluoride salts were also proposed as potential coolants for blanket modules in fusion reactor designs.[43, 44] A fusion reactor blanket—no matter what type of fusion reactor—generally has three requirements: (1) remove heat generated by fusion reaction, (2) generate tritium to replace the amount used by the fusion reaction, and (3) shield structural materials from the neutron field generated by the plasma. Fluoride salts are very attractive candidates for

[b] Context comment: The statements on "current" efforts are dated to 2017. Since then, the two university-led projects noted have ended, but several new university efforts have started with support from DOE-NE. Internationally, MSR concepts are still being pursued; the reader is referred to more recent literature, press releases, or working groups such as those in the Gen-IV International Forum.

[c] Context comment: The list of companies actively developing or exploring molten salt reactors in 2023 has expanded to include Kairos Power, Natura Resources, Exodys Energy, Moltex Energy, ThorCon, Copenhagen Atomics, Seaborg Technologies, Naarea, Thorizon, and Alpha Tech Research Corp., among others. Key recent highlights include construction permit applications to the US Nuclear Regulatory Commission by Kairos Power for the Hermes molten salt-cooled test reactor and Abilene Christian University for the Molten Salt Research Reactor. In addition, DOE's Advanced Reactor Demonstration Program selected Southern Company and subrecipient TerraPower to design, construct, and operate the Molten Chloride Reactor Experiment (MCRE).

meeting the first two of these requirements. Liquid fluoride salts have favorable thermal transport properties and therefore good heat transfer characteristics: they can effectively fulfill the heat removal requirement. The second requirement can be addressed by introducing lithium into the blanket design, with tritium produced by neutron capture. To improve tritium production, beryllium is also often introduced. FLiBe salt is often proposed as a potential blanket coolant, although other salts remain attractive[45] for tritium production. Although the salt itself is not an effective neutron absorber, it is very stable in a neutron field and is an effective shield component coolant.

Various designs of liquid salt–based tritium breeding blankets have been proposed. Some designs use the salt only for breeding,[46] and some use the salt both to breed tritium and as a high-temperature heat-transfer medium to remove blanket heat for power production.[47] Conventional fluoride salt breeder blanket designs use a circulating fluoride salt inside a breeding blanket structure. For the two-fluid concept, the salt is used only for tritium breeding, and helium is often proposed for removing most of the plasma-generated heat.[46] However, some novel liquid salt blanket designs have been proposed that use a liquid fluoride salt "waterfall" facing the plasma.[48] In this concept, the liquid actually forms the plasma-facing wall and is used to absorb first-wall surface heating. Another concept proposed by Lawrence Livermore National Laboratory dissolves thorium in the breeding salt to produce ^{233}U and tritium.[49, 50] The ^{233}U would be used to fuel the fission reactor fleet and would provide an additional revenue stream for the fusion reactor.

Fluoride salts have also been proposed as thermal storage media, making use of the salt heat resulting from fusion to provide a low mass/volume storage media. Misra and Whittenberger examined a variety of fluoride salt eutectics, congruently melting fluoride salts to determine their usefulness as a storage medium for solar space power applications.[51] Their study analyzed a variety of fluoride salts with melt temperatures ranging between 973 K and 1,400 K and heat of fusion ranging between 0.44 and 1.08 kJ/g. Fluoride salts have also been proposed as storage media using only their sensible heats. The small fluoride salt-cooled high temperature reactor (SmAHTR) concept utilized a salt vault to couple multiple reactors.[25] The proposed storage used the sensible heat of either liquid FLiNaK (46.5% LiF, 11.5% NaF, 42% KF) or NaF-$NaBF_4$ (8% NaF, 92% $NaBF_4$) salts operating between 500°C and 600°C to supply process heat or heat for a power conversion system from multiple FHR type reactors.

Development of fluoride salt systems will require (1) reinitiating salt experimentation to recapture expertise that has been lost over time, (2) extending the research that was carried out in the various programs discussed above to adapt new reactor designs and licensing requirements, and (3) integrating new technology that has been developed in the intervening years that will make the new fluoride salt reactor designs more robust and economical.

As a first step in this process, ORNL designed and constructed a versatile forced convection fluoride salt loop to help address practical issues associated with these reactor designs. A hydrogen fluoride–hydrogen based salt purification system is used to preclean the salt before it is introduced into the experiment loop. This paper highlights some of the issues and successes observed during the start-up of this facility.

3. LOOP DESCRIPTION

LSTL is a small forced-convection test facility providing a versatile experimental platform for separate effects and component testing. A schematic of the loop is shown in Figure 1. The facility uses 150 kg of FLiNaK salt and is designed to operate at temperatures up to 700°C. An Ar cover gas at a few kPa (i.e., just above atmospheric pressure) is used to maintain an oxygen- and moisture-free atmosphere over the salt. A 150 L storage tank allows the salt to be frozen for long-term storage. The storage tank heating provides three separate heating zones that allow the frozen salt to be thawed from the top to the bottom, thus preventing the salt from expanding as it thaws and overstressing the tank. Instrumentation in the storage tank is capable of measuring the tank's salt level, salt temperature, and gas pressure. A gas pressurization and let-down system for the storage tank is used to maintain an Ar overpressure on the salt and to move salt between the storage tank, the loop, and the salt clean-up system. A second surge tank at the top of the loop is used as an expansion tank, operating with a liquid-vapor interface to ensure that the loop is completely filled with salt. This tank also includes instrumentation capable of measuring the tank's salt level, gas pressure, and salt temperature. A gas pressurization and let-down system is also included. An air-cooled finned-tube heat exchanger is used to remove heat from the loop. The heat exchanger contains fourteen 2.54 cm diameter finned tubes and is air-cooled by a variable speed fan system.

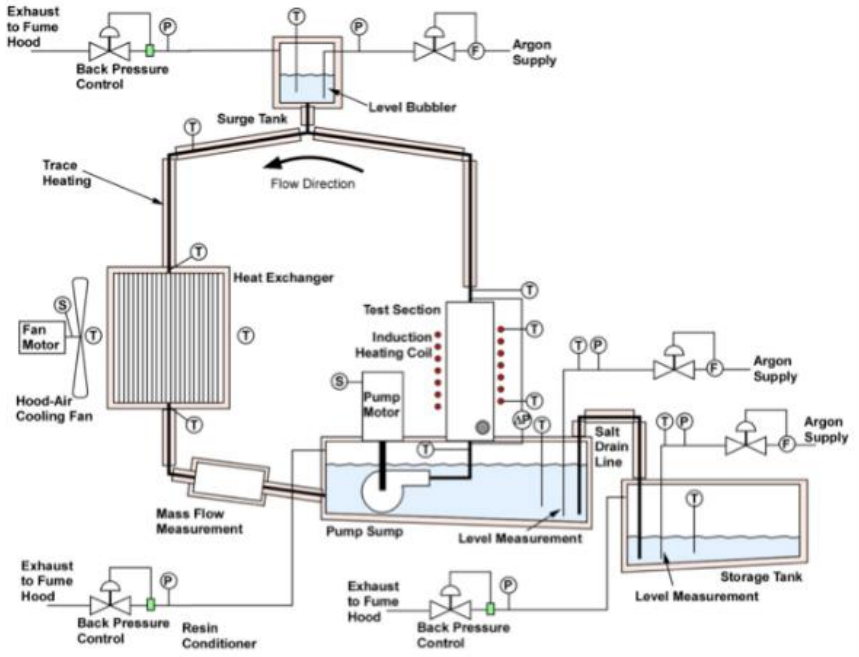

Figure 1. LSTL schematic.

The LSTL includes a small centrifugal pump with a design flow rate of 4.5 kg/s of salt at 0.125 MPa pump head. The pump is driven with a 10 horsepower motor and variable frequency drive for pump speed control. The pump uses an overhung impeller and is housed in a sump tank. Like to the surge tank, the sump tank operates with a salt–Ar interface and includes instrumentation capable of measuring tank salt level, gas pressure, and salt temperature. A gas pressurization and let-down system is also included. The sump tank also contains the piping connecting the pump and the test section. A salt pressure measurement transducer is included in the pump outlet piping.

The initial tests conducted in the LSTL were designed to examine the heat transfer that will occur in the core of the PB-AHTR,[26] a reactor design that uses a solid pebble fuel cooled by FLiBe salt. The initial LSTL test section is designed to measure pebble bed heat transfer to a flowing fluoride salt. A unique inductive heating technique is used to heat the pebbles. The 24 cm long induction coil surrounds a SiC flow tube. The SiC tube is nearly transparent to the induction field and houses a 15 cm diameter graphite pebble bed. The 3 cm diameter graphite pebbles act as a susceptor for the magnetic field of the induction heater. Pebble powers ranging up to about 1.25 kW/pebble can be provided by the 200 kW induction heating system. A photo of the pebbles during loading into the SiC tube is shown in Figure 2.

Figure 2. Pebbles shown during loading into the SiC test section.

Two of the pebbles are instrumented with thermocouples located at their centers. Companion thermocouples are located adjacent to the instrumented pebbles to provide fluid temperatures at the pebble location. One of the instrumented thermocouples is located as near to the radial centerline of the test section as possible, and the second pebble is located about halfway between the radial centerline and the SiC flow tube inner wall. Both pebbles are located at the axial centerline of the induction coils. In addition to the thermocouples included for pebble thermometry, one thermocouple is located at the inlet of the test section to measure the salt inlet temperature, and two additional fluid thermocouples are located at the test section outlet. Table 1 provides a summary of loop capabilities.

Table 1. Loop design conditions

Property	Value
Salt	FLiNaK
Operating temperature	700°C
Flow rate	4.5 kg/s
Operating pressure	Atmospheric
Material of construction	Alloy
Loop volume	72 L
Bed diameter	15 cm
Bed height	0.75 m
Pebble diameter	3 cm
Reynolds number	2,570

An ultrasonic flowmeter is used to measure FLiNaK flow in the test section. A combination of heating blankets, heating tape, and tubular heaters is used to maintain loop temperatures above the FLiNaK freezing point of 454°C. All components have heating systems, including the heat exchanger, which has a combination of tubular heaters and insulated doors to maintain temperatures above the freezing point. A picture of the loop is shown in Figure 3, and additional information about the LSTL design can be found in the literature.[51–54]

Figure 3. Liquid salt test loop.

This facility contains several novel design features and components not previously used in high-temperature fluoride salt systems. The pump is a conventional overhung centrifugal impeller design. However, it includes a dry gas non-contact rotating shaft seal which is used to isolate the sump tank from the atmosphere. The design uses a commercial seal manufactured by John Crane. This seal, shown in Figure 4, has a very low leak rate, but it also has very high tolerance requirements. If a dry gas seal can be shown to be usable, then many of the problems that occurred with the MSRE pump,[55] such as oil leakage into the salt cover gas, can be avoided.

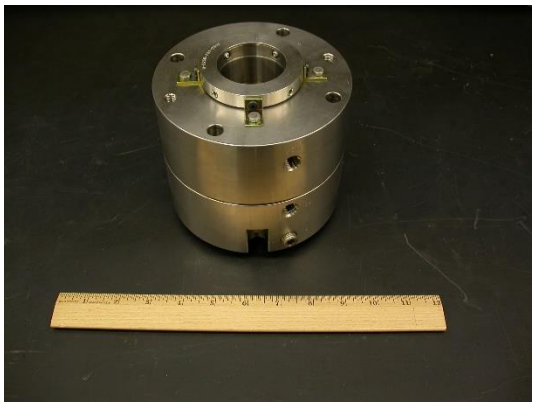

Figure 4. John Crane rotating shaft seal.

The LSTL also uses a two-seal system to connect the SiC test section's upper flange to the Alloy 600 loop piping and to ensure that air leakage into the loop is not possible. This design consists of an inner Flexitallic spiral wound (grafoil/Ni) gasket that is in contact with the salt. An outer Parker C-type seal is used to provide a volume between the two seals where Ar is maintained at a pressure above that of the loop's pressure. Because both seals must be compressed, and because there is a large difference between the thermal expansion coefficients of SiC and Alloy 600, a significant amount of engineering was needed to develop a seal system design that not only sealed properly, but that also would not break the SiC test section.

A similar seal system is used on the adjustable joint flange located in the piping between the test section and the surge tank. The adjustable joint allows the pipe to accommodate some variation in the location of the test section upper flange assembly. The schematic of the two-seal design is shown in Figure 5.

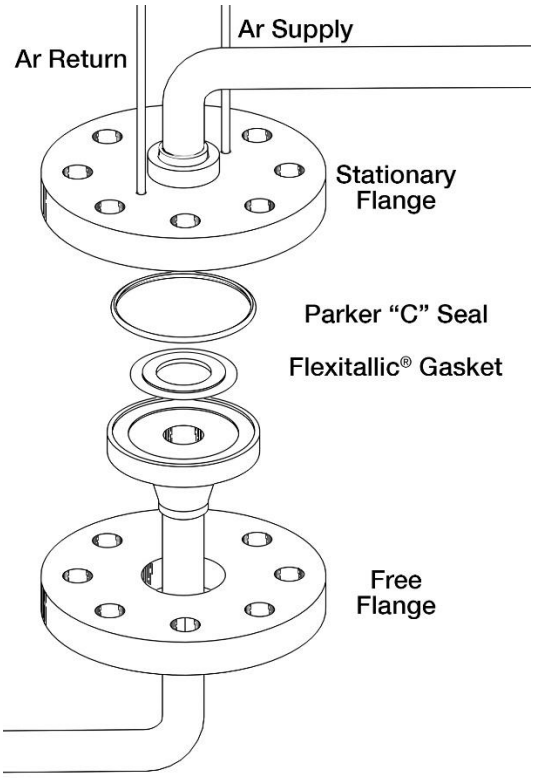

Figure 5. Schematic of double seal design.

Two points in the loop are fixed in space: the top of the test section, and the bottom of the sump tank at the centerline of the test section. This design was selected to minimize stresses on the SiC flow tube. The design required the sump tank to be capable of vertical movement with respect to the SiC flow tube as the component temperatures changed. Fixing the top of the test section and the bottom of the sump tank also allows the compliant seal to be located in the gas space in the sump tank and only requires that the seal be able to prevent gas leakage. A three-piston ring design was chosen to allow the SiC to move vertically relative to the pump sump tank while minimizing gas leakage (Figure 6).

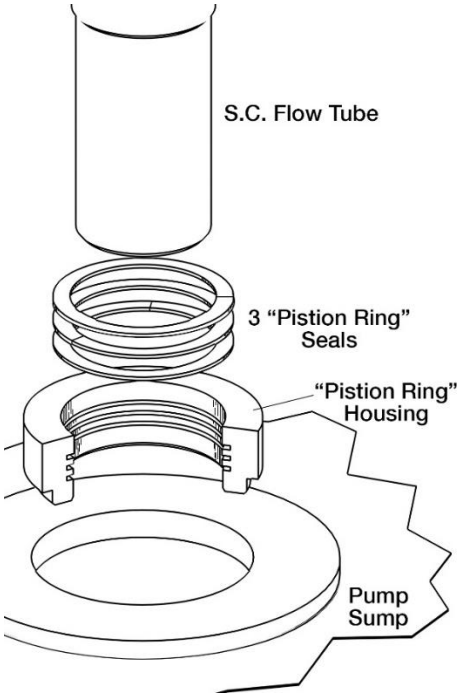

Figure 6. Schematic of three piston ring–seal design.

Several novel high-temperature instruments were installed in the loop: the ultrasonic flowmeter purchased from FLEXIM, and a NaK-filled pressure transducer produced by GP-50. A Vega radar-based level detector was also installed in the pump sump tank. These instruments are shown in Figure 7. Operational experience with these instruments is described in Section 5.4 below.

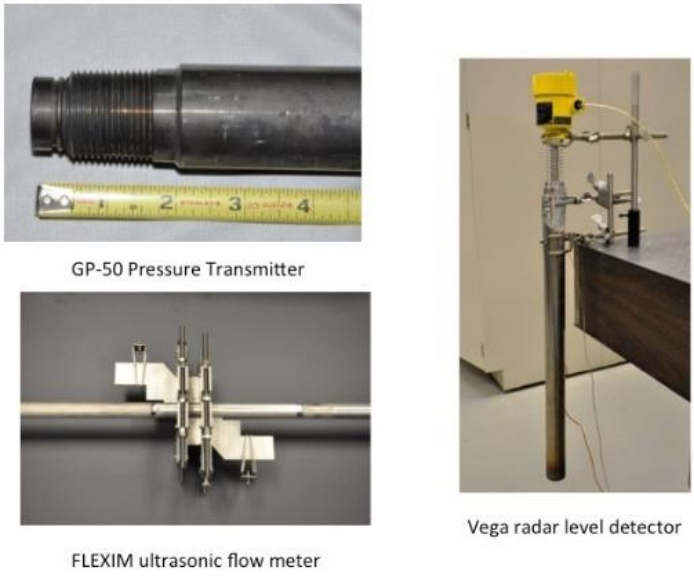

Figure 7. High-temperature instrumentation.

4. FLUORIDE SALT PURIFICATION SYSTEM DSCRIPTION

Commercially available fluoride salts contain a variety of contaminants, including tramp metals, sulfur, moisture, and oxides. Contaminants in the salt cause corrosion on structural materials and must be removed to minimize corrosion and ensure acceptable equipment lifetime.

A salt clean-up system was built to support LSTL operation. The design is based on the hydrofluorination process that was developed for and used to supply fluoride salt for MSRE.[14] The process uses anhydrous hydrogen fluoride (HF) and hydrogen bubbled through liquid fluoride salt. Argon is used in the processing step as a sweep gas to ensure that HF and hydrogen do not accumulate within the crucible system, and once processing is complete, Ar is used to remove all HF and H_2 from the system.

Processing consists of several steps. FLiNaK is initially mixed in the appropriate proportions from the individual solid components. Once the salt is mixed, it is poured into the Ni crucible, and the vessel is closed. Dry Ar is introduced through the dip tube and into the void space above the powdered salt. The heating blanket and tubular heater at the bottom of the vessel are used to increase the crucible temperature in ~100°C increments to remove moisture from the salt. Once drying is complete, the salt is raised to the melting point (454°C) and finally to the 600°C processing temperature. The drying/melting process takes 1–2 d to complete. H_2 and HF are then introduced through the bubbler tube, and the hydrofluorination process continues for approximately 3 d. At that point, the HF is shut off, and the H_2 flow continues for another day to reduce any metal fluorides that might have accumulated in the salt. Argon is then introduced into the bubbler gas line, and another day of operating with 100% Ar ensures that all HF and H_2 have been removed from the system before the salt transfer tube is installed.

The purification system consists of three major components: (1) a gas supply system, (2) a processing crucible, and (3) an exhaust gas scrubber system.

4.1 PROCESSING CRUCIBLE

The fluoride salt purification crucible consists of an inner Ni vessel that is used to contain the salt, and an outer stainless-steel vessel is used to maintain the proper atmosphere above the salt. The Ni crucible is 183 cm tall and 43 cm in diameter and can process approximately 160 kg of salt at a time. The upper flange of the outer stainless-steel vessel contains four port tubes that terminate in Swagelok® compression fittings. The tubes are long enough to significantly reduce the compression fitting temperature to well below the process temperature, thus preventing the connection from seizing. One of the ports contains a ¼ in. (6.35 mm) Ni tube that runs to the bottom of the crucible and acts as a bubbler to carry the process gas (3 slpm of H_2 and 0.3 slpm of HF) to the bottom of the salt melt. A second port is used to supply 3 slpm of Ar sweep gas across the top of the crucible to ensure that process gasses do not accumulate in the crucible. The third port is used as the crucible system's exhaust. During the salt heat-up/drying and melting process phases, the fourth port is used to house an Omega thermocouple rake with six axial thermocouple positions to measure the salt temperature and to determine when the salt is melted and at what processing temperature. This thermocouple probe is removed after melting, prior to HF processing. After HF processing is complete, the port is used to install a ½ in. (12.7 mm) salt transfer tube to transfer purified salt from the processing crucible to the LSTL storage tank. A schematic of the crucible is shown in Figure 8, and a picture of the system is shown in Figure 9.

The crucible is heated using a HTS/Amptek blanket heater that surrounds the perimeter of the stainless-steel vessel. The blanket has three axial heater zones with a total power of 10 kW to allow remelt of the salt in the event that it freezes in the crucible. An ASB Heating Elements Ltd. 1.5 kW tubular heating element is attached to the bottom of the crucible.

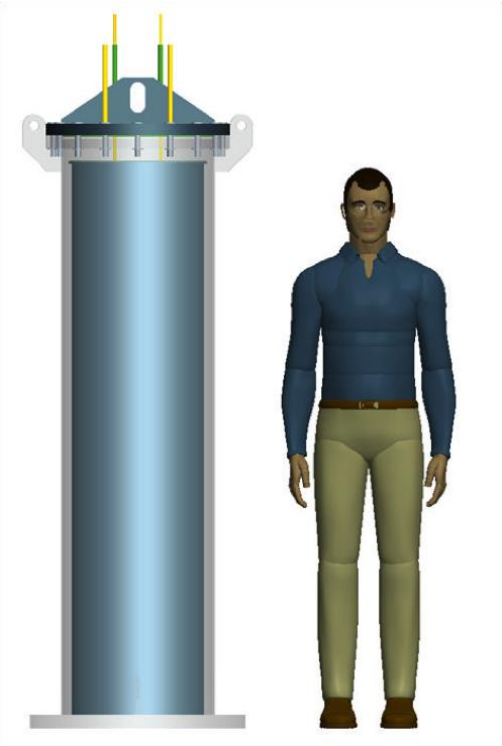

Figure 8. Processing crucible relative size.

Figure 9. Installed purification crucible.

4.2 GAS SUPPLY SYSTEM

The gas supply system is used to supply the three gases used in the process. A schematic of the gas supply system is shown in Figure 10. The hydrogen system uses three hydrogen gas bottles and consists of a pressure regulator, a particulate filter, a column to remove any oxygen from the supply gas system, and a mass flow controller. An air-to-open emergency shutoff valve is used in the hydrogen supply to allow rapid shutoff of the hydrogen in case operating parameters get out of range.

The Ar supply system is similar to the hydrogen system, except it includes two mass flow controllers—one to control Ar going through the salt bubbler tube, and one to control sweep gas across the top of the crucible. The Ar system does not include an emergency shut-off valve.

Hydrogen fluoride is a liquid at normal temperature and pressure. The HF must be heated to produce enough HF gas pressure to flow through the cleanup system. A heating blanket is used to heat the HF bottle to approximately 38°C, and heating tapes are used to maintain all piping temperatures containing HF above the condensation point. A mass flow controller is used to meter HF flow, and an air-to-open emergency shutoff valve is used in the HF supply line.

A vacuum system is used to allow tubing to be evacuated and then purged during bottle replacement. The vacuum system is capable of removing all H_2 and HF from the tubing if components need replacing. Operating parameters for the system used to supply clean salt for the LSTL are shown in Table 2.

4.3 EXHAUST SCRUBBER SYSTEM

During processing, the exhaust stream from the crucible can contain Ar, H_2, and HF gases. The HF is stripped from the gas stream by running the exhaust through a water bubbler system. The system consists of four plastic carboys. The first acts as a vacuum break and prevents any water in the following vessels from flowing back to the processing crucible if a vessel depressurization should occur. The next three carboys are all the same, consisting of a bubbler tube that extends to the bottom of each vessel, forcing exhaust flow to bubble through ~3.8 L of water. The three water bubblers are in series, and all vessels are submerged in a tank filled with water to avoid the possibility of a leak, which could cause a H_2 fire and melt the plastic containers and tubing. Because HF gas is rapidly absorbed in water, forming hydrofluoric acid, the bubbler system removes all HF from the exhaust stream. Because all of the tanks and plastic piping are submerged under water, the HF would be stripped from the gas stream in case of a leak. The remaining Ar and H_2 are discharged into the hood through a flame arrestor and then to the environment. A picture of the bubbler system is shown in Figure 11.

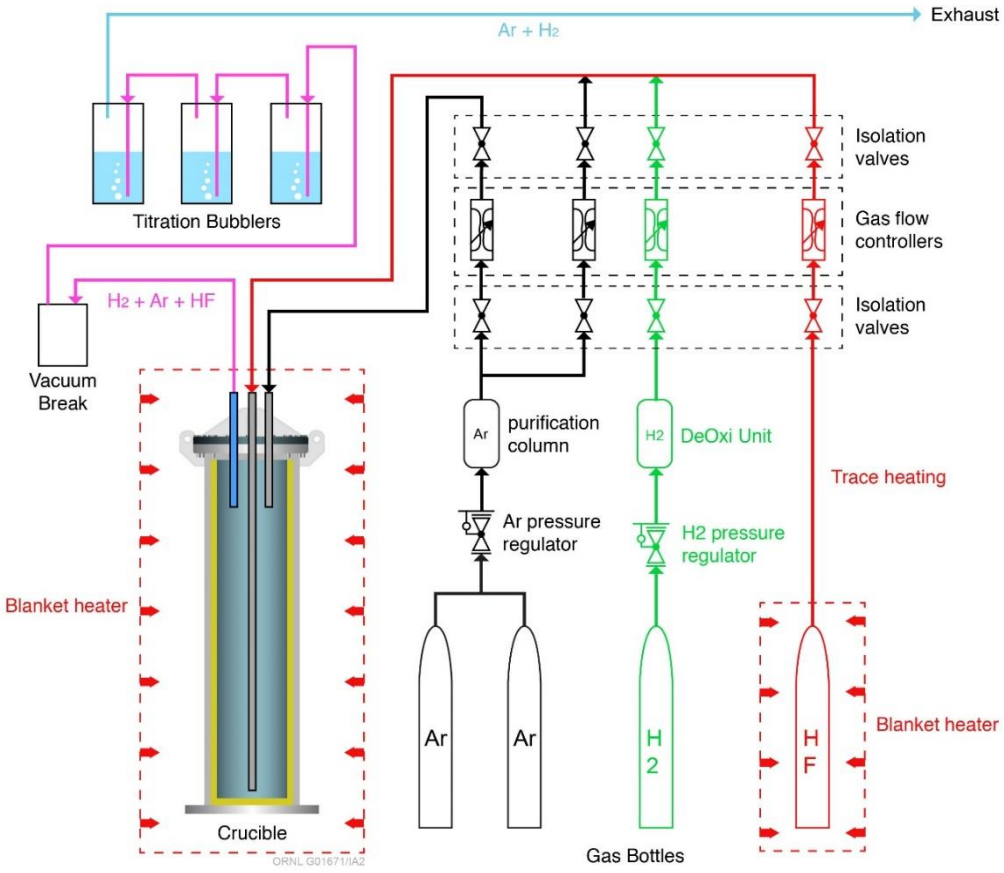

Figure 10. Gas supply system piping and instrumentation diagram.

Table 2. Salt cleanup system parameters

Parameter	Value
Salt capacity	160 kg
Ar flow rate Bubbler Sweep	 3 slpm 3 slpm
H_2 flow rate	3 slpm
HF flow rate	0.3 slpm

After the liquid salt is purified, it is transferred from the crucible to the storage tank using pressure differentials via a Ni transfer tube that extends to the bottom of both tanks. The transfer tube includes a 25 μm filter from Porous Metal Filters that is used to remove residual particulate from the salt. The filter and housing is pictured in Figure 12.

Figure 11. Salt clean-up exhaust water bubbler system.

Figure 12. Salt transfer line filter.

5. START-UP SYSTEM EXPERIENCE

5.1 SALT CLEAN-UP SYSTEM OPERATION

Commercial quality salts—KF, NaF, and LiF—were purchased from Alfa Aesar to make 150 kg of FLiNaK. Salt was purchased over 5 years before actual system operation. Each salt component was weighed and poured into an 8 L plastic carboy for mixing. The melting temperature for each individual salt component is higher than the upper temperature limit of the processing crucible, so mixing is needed to ensure that the eutectic melting point is achieved. To leave sufficient space for mixing, approximately 3 kg of salt was placed in each carboy. During the loading process, it was found that a significant amount of the KF salt had absorbed moisture and hardened to the point that it had to be chipped apart to be weighed and loaded into the carboy. Because this process proved very tedious, a new batch of anhydrous KF salt was purchased from Alfa to avoid the labor associated with breaking the KF apart. The new batch was ordered in 1.77 kg bags, which is the approximate amount needed for one carboy. Even the fresh salt had some solid lumps that had to be broken apart to ensure adequate mixing in the carboy.

After being filled with salt, each carboy was loaded with twelve 2.54 cm diameter stainless-steel balls and placed in a ball mill for approximately 1 h for mixing (See Figure 13). Notably, once the KF was mixed with the other salts, loaded in the carboy, and the cap installed, no obvious clumping problems were observed, even for the salt that remained in the carboys for several more months.

Figure 13. Three carboys loaded with salt in the ball mill.

After the salt was mixed, it was poured from the carboys to the crucible through a screen to remove stainless balls. The crucible was loaded with salt up to about 10 in. (0.25 m) below the top of the Ni liner, as shown Figure 14.

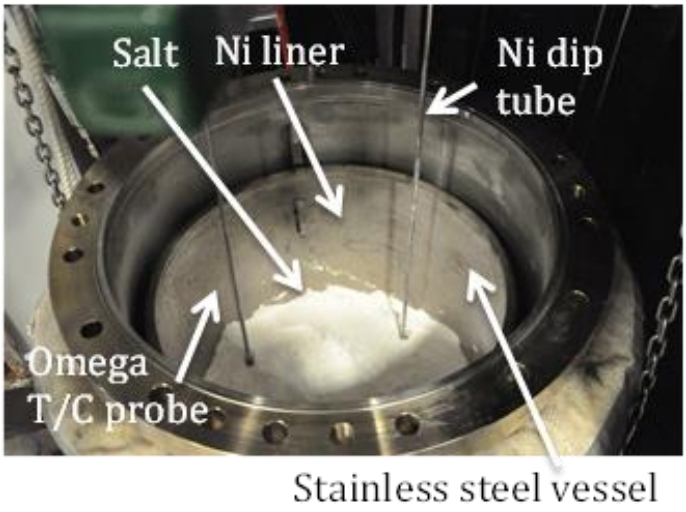

Figure 14. Salt loaded into purification vessel.

After the crucible was filled, the crucible flange sealing surfaces and Parker seal were thoroughly cleaned with acetone and then alcohol to assure a good seal. The crucible flange bolts were then torqued to achieve the proper seal loading. Both the bubbler tube and salt thermocouple probe were installed in the crucible before the salt was loaded to avoid problems inserting them through the 6 ft (1.83 m) depth of salt powder after loading.

The entire salt purification process was scheduled to last approximately 7 d; however, several problems occurred that caused the process to take significantly longer. The process was started by flowing 3 slpm of Ar through the sweep region of the crucible and 3 slpm of Ar through the bubbler tube. The crucible heaters were then turned on, and the crucible temperature was increased in increments of ~125°C and held for ~24 h at each temperature. At several periods during the drying process, the clear plastic exhaust tubing appeared to have fogged with condensed liquid on the inner surface. Droplets appeared on the tubing's inner surface even as the salt was melting. A picture of the droplets in the exhaust tube is shown in Figure 15. The Omega thermocouple probe indicated that the salt powder melted at about 468°C. After melting, the salt temperature was raised to the final processing temperature of 600°C.

Figure 15. Droplets in crucible exhaust line.

HF and H_2 were then introduced into the crucible dip tube to begin processing. The system operated for about 3 h, and the HF mass flow controller began to give erratic readings. The HF and H_2 flows were halted, and after investigation, it was determined that HF had condensed in the mass flow controller. Once the problem was identified, the temperature setpoints for the HF trace heaters were increased, additional insulation was added, and the HF mass flow controller began to work again. HF and H_2 flows were reinitiated, and the processing continued. During operation, the crucible exhaust line pressure slowly increased during a period of about 20 h of operation, indicating that the exhaust line was slowly being blocked. The system gas flows were also reduced during this time to keep the exhaust pressure under 21 kPa (3 psig), a pressure level that was judged to be low enough to prevent failure of the plastic piping and tanks. Also during this period, a black layer began to form inside the clear plastic exhaust tubing that was first noticed at the inlet line to the vacuum break tank in the exhaust scrubber system. Some of the black material could also be observed floating on the top the bubbler water. Post-processing elemental analysis indicated that this material was mostly KF with some trace quantities of metals, indicating that KF vapor from the salt must have recondensed in the cooler portions of the exhaust lines. After about 20 h of operation, the increased pressures could no longer be controlled by reducing gas flows, and the HF and H_2 flows were terminated. Once the HF and H_2 were completely swept from the system with Ar, the scrubber system was bypassed. On examination, it was determined that the flash arrestor used at the discharge of the scrubber system was blocked with what appeared to be a black powder. Post-test analysis of this material also indicated that most of the material was KF that apparently had made its way through the water bubbler system.

A modification to the scrubber exhaust included three flash arrestors plumbed in parallel. The design allowed each flash arrestor to be individually valved into or out of the scrubber exhaust so that when one plugged, another fresh arrestor could be valved into the exhaust flow. This configuration allowed processing to continue to completion. The total elapsed time (including periods to investigate and correct problems) from the start of HF/H_2 flow until the process was determined to be complete was about 21 d. During this entire period, the crucible temperature was maintained at 600°C.

Once the HF/H_2 processing was complete, the salt transfer tube was installed between the processing crucible and the loop salt storage tank. The transfer line included a 25 μm filter to remove residual particulate from the salt. During the salt transfer, which took approximately 6 h, the pressure differential between the crucible and the storage tank increased, indicating that restriction in the filter was increasing. After the transfer the filter was removed (Figure 16), the material captured by the filter was analyzed. The elemental analysis indicated that the material was composed of a significant amount of potassium and trace quantities of nickel, iron, and chrome.

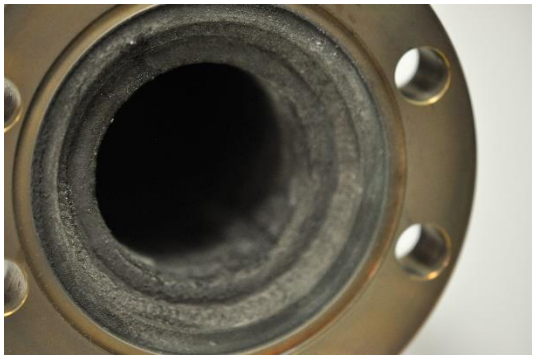

Figure 16. Filter after removal from transfer line.

SiC to Alloy 600 seal performance. As discussed above, the SiC test section includes a double ring seal at the top flange face and a piston ring seal between the sump tank and the tube. From the top to the bottom, the top flange assembly consists of an Inconel 600 flange, two seals, the SiC flange, and finally, an Inconel 600 backing ring. Inconel 718 bolts extending through the metallic upper flange and backer ring are used to compress the assembly. To accommodate differential thermal expansion between the bolts and the SiC flange, a stack of four Belleville washers are included with each bolt.

During the initial installation of the SiC test section, the SiC flange fractured. The lubricated bolts and nuts were being tightened one at a time using a manual torque wrench. The tightening sequence followed a typical cross pattern. A relatively high, near-final torque was being applied to each bolt, and near the completion of the tightening pattern, a loud sound was heard. It was difficult to observe the crack in the black SiC flange in situ because of the flange arrangement, but the crack was clearly visible on disassembly. The failure occurred across the SiC flange face and across a portion of the tube section. The failure of the first SiC test section and an unrelated delay in the project schedule motivated three activities: resurfacing of the backing ring, redesign of the upper flange support, and testing with dummy SiC flange assemblies.The flatness of the backing ring plate was rechecked, and then the surface was then reground to a flatness of 12.7 μ.

In the original setup, the backing ring plate was mounted to the frame holding the sump tank. The SiC flange was then held between the backing ring plate and the circular upper flange. A pipe was attached to the upper flange through which the salt exits the test section. Stresses on this pipe from thermal expansion during heat up or cooldown of the loop would be translated onto the SiC flange. To avoid this loading, the flange arrangement was redesigned. In the new arrangement, the upper flange is bolted to the frame, and the backing ring plate is used to tighten the SiC flange to the upper flange. In this configuration, loading on the upper flange is translated directly to the frame and not through the SiC flange.

A series of tests was performed in which dummy SiC flanges were installed, instrumented, insulated, pressurized with Ar, heated, cooled, and leak checked. The dummy flanges had the same flange geometry as the SiC test section, but it included a shorter tube section with a closed bottom. A photo of the test setup without the insulation is provided in Figure 17.

Figure 17. SiC flange test assembly with thermocouples and trace heaters installed (before insulation is added).

These tests guided the torquing procedure, the final gap spacing between the SiC and upper flange, the heater requirements, and the thermocouple attachment techniques. The inner Flexitallic spiral-wound graphoil seal was found to readily seal at low compression. The outer metallic C-ring seal had a much higher leak rate that improved with increasing temperature. The testing also motivated two changes. As originally designed, the top flange and SiC flange were to be fully compressed such that a land on the upper flange would contact the SiC flange. In practice, it was found beneficial to leave a gap between these two surfaces. The second change was to include a ring of Thermiculite™ 815 gasket material between the backing ring and the SiC flange. This provided some compliance between the two surfaces. Ultimately, these changes and insights led to the successful installation and operation of the SiC test section.

During operation, the flow and pressure of gas into the space between the inner and outer seals of both the SiC flange and the rotating flange are monitored and controlled. Gas flow and pressure to both flanges are controlled by shared inlet and outlet gas mass flow controllers. Over 2 d of loop operation, the system added approximately 1.75 slpm of Ar. This suggests a total gas leak rate of the two flange locations—including connections and valves in the piping—of 0.0006 slpm. Although this performance is quite promising, extended flange operation and future disassembly will provide more definitive findings.

The piston ring seal between the SiC test section tube and sump tank also performed quite well. The piston rings would seat and the leakage rate would decrease after the sump tank was sufficiently pressurized. With salt in the sump tank and the pump operating, the leak rate in the sump tank was approximately 0.8–1.5 slpm at 46 kPa (6.7 psig). This was much lower than the anticipated leakage rate of approximately 23–26 slpm at 207 kPa (30 psig) at temperatures of 500–700°C. The seal leakage also decreased with increasing temperature, as expected.

5.2 LOOP OPERATION

The planned startup of the loop included the following major steps:

1. purification of the salt,
2. hydrogen firing of the storage tank (4% H_2, 96% Ar) during initial heat up,
3. transfer of salt from the crucible to the loop storage tank,
4. hydrogen firing of the loop system during initial loop heat up,
5. loop fill via the transfer tube from the storage tank,
6. operation of the pump to circulate salt through the loop, which also serves to clean the loop,
7. operation of the induction power supply and coil at low power,
8. transfer of salt back to the crucible for purification, and

9. transfer of salt back to the loop for heat transfer tests.

Operations were completed through step 7. Funding limitations prevented completion of steps 8 and 9 at the initial development of this report.

The thermal management system comprises a large part of the instrumentation and controls system. There are 25 heater zones between the loop and purification systems. The storage tank, sump tank, surge tank, and crucible are heated using custom fabricated heater blankets. The bottom of the crucible and sump tank and the front and back faces of the heat exchanger use tubular heating elements. Piping legs, the SiC test section, and flanges use heating tape.

Heater power to each zone is controlled using proportional-integral-derivative (PID) feedback from a thermocouple input with a software-controlled output function. Heater power output is varied using solid-state relays to turn the power on or off. PID feedback loop output controls the percentage of time that the heater is turned on over a 10 s period to maintain the target temperature.

The initial heat-up of the loop was intended to verify that the temperature could be maintained well above the melting temperature of the FLiNaK salt (456°C) before moving salt into the loop. Temperature indicators showed cold spots in the heat exchanger and in the piping at the externally mounted flowmeter location.

The heat exchanger indicated temperatures in the corner regions as low as 400°C. For this initial circulation and cleanup phase, the insulated doors were closed over the front and back faces of the heat exchanger. Additional insulation was added around the edges of the door, but this did not increase the temperatures sufficiently. The original design included tube-type heating elements on both faces of the heat exchanger, rated at 750 W each. These heating elements were replaced with 2 kW heaters on both sides. Subsequent heat-up indicated that the lowest temperatures were at just under 500°C with these heaters at full power.

The FLEXIM ultrasonic flowmeter is attached to the outside of the 25 mm (1 in.) pipe, as shown in Figure 18. The waveguides and associated hardware can be seen in the photo, along with the trace heaters wrapped around the pipe. The configuration shown was insulated about halfway up the waveguides to allow the electronics (not shown) to remain cool, but temperatures of the pipe were observed to be as low as ~300°C. The density of the wrapped trace heaters is limited by the hardware geometry and did not provide sufficient heating.

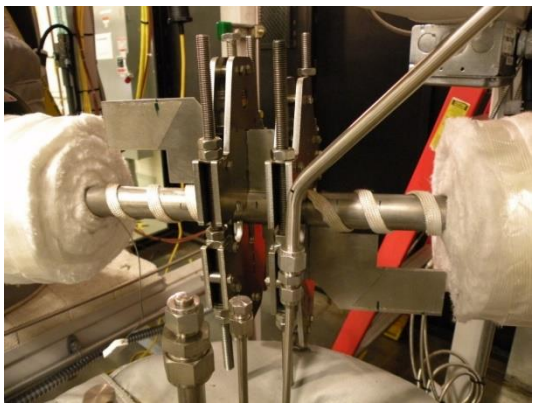

Figure 18. FLEXIM ultrasonic flowmeter installed on loop piping (shown with insulation removed).

As mentioned in step 6, the initial circulation of salt through the loop components was intended to use the salt itself to further clean the internal surfaces. A flow measurement was not necessary for this purpose, so the insulated flowmeter region was wrapped with additional trace heaters and insulation sufficient to bring the pipe to a temperature to allow loop fill and salt circulation. The long-term plan is to clamp cartridge heaters on the pipe in the flowmeter region to increase pipe temperature. It is yet to be determined whether active cooling of the waveguides where the electronics attach will be necessary.

With the loop at a high enough temperature to support molten salt operation, and with the salt molten in the storage tank, the transfer tube between the two tanks was installed. The transfer tube is u-shaped and extends to the bottom of both tanks when fully inserted. To insert the tube, the transfer tube ports that were made of bored-through Swagelok fittings were opened, and an Ar gas purge was maintained to prevent ingress of air into the vessels during installation. The transfer tube was also purged with Ar gas from one end up until just before it was lowered into the port on the tank. As the tube was initially lowered into the vessels, the gas spaces in each tank were connected by the open tube. When the tube end reached the liquid level in the storage tank, this was no longer the case. During the first attempt at inserting the transfer tube, the Swagelok fitting on the storage tank port partially sealed without being tightened, and the purge gas was no longer sufficiently vented. This created a higher pressure in the storage tank and pushed salt into the cold transfer tube, where it froze part way up the tube. For later insertions and removals, a separate vent path for the storage tank and sump tank was opened to prevent inadvertent movement of salt into the transfer tube. A photo of the insulated transfer tube installed between the two tanks is shown in Fig. 19.

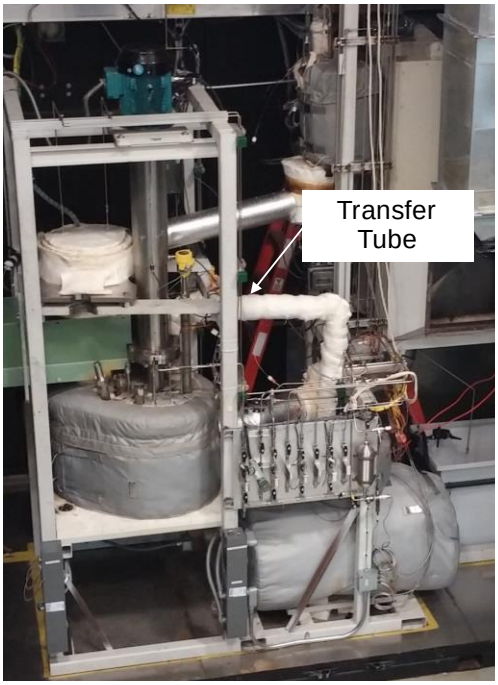

Figure 19. Transfer tube installed between storage and sump tanks.

Figure 19 shows the transfer tube installed in the loop. After the transfer tube was inserted, the salt was moved into the sump tank by using gas pressure applied to the storage tank. When the pressure differential between the storage tank and sump tank was large enough to raise the salt to the top of the transfer tube, salt began to flow from the storage tank to the pump sump tank. Once the storage tank emptied, the salt could be raised in the loop by increasing in storage tank pressure. This process can be followed by examination of pressure traces in the different tanks during the fill operation.

A screenshot of the gas control system operator display illustrating the controls available to the operator is shown in Figure 20. Mass flow controllers and a solenoid valve (for the sump tank vent) are used to supply and vent gas from the storage, sump, and surge tanks. The mass flow controllers can be operated individually in manual mode or automatically in feedback mode to control the corresponding vessel pressure.

An example of the pressure measured in the three vessels during the loop fill and subsequent pump operation is illustrative of the control methods used to perform these operations (Figure 21).

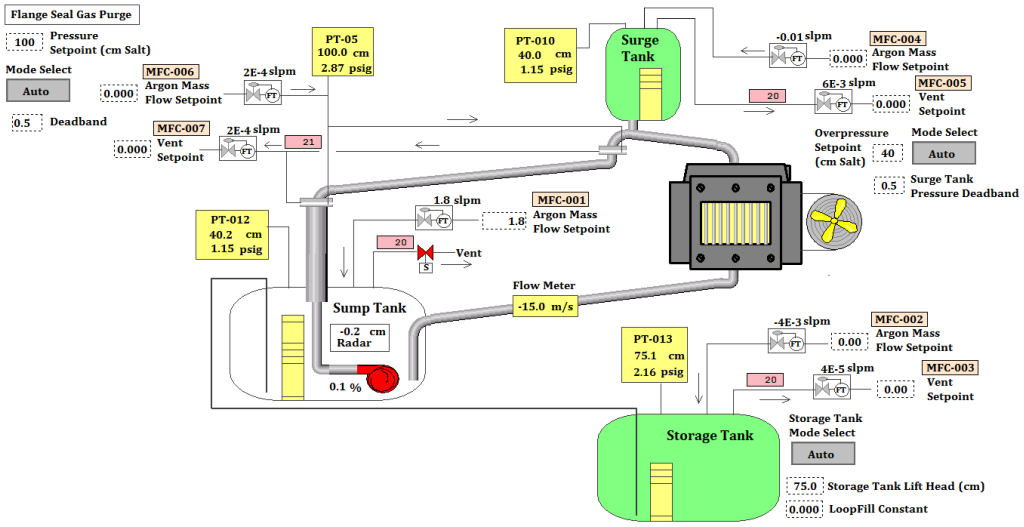

Figure 20. Screen shot of gas control system operator display.

Note that the units of pressure are in centimeters of salt head (relative to atmospheric pressure). Because many of the operations involve movement of salt into and out of the loop and are controlled by the salt head, these units are convenient for operators. Initial pressures shown in Figure 21 are at the nominal levels maintained when the system is left unattended in a hot standby condition. At the beginning of this process, the salt was in the storage tank. The sump tank and surge tank were connected by the gas-filled loop piping and were at the same pressure (PT-010, surge tank pressure in blue hidden by the orange sump tank pressure, PT-012). To initiate the salt transfer process, the pressure was reduced on both sides of the transfer tube by venting gas while maintaining a higher pressure on the sump tank side. When the storage tank pressure reached ~100 cm of salt head, venting was stopped. The surge tank pressure control was set to automatic, and the overpressure set point was 60 cm of salt. The storage tank controls were set to automatic, and the set point was increased in steps to 210 cm of salt head. Up until this point, the surge tank and sump tank were still at the same pressure. As the storage tank pressure was increased above this value, the sump tank pressure began to separate from the surge tank pressure, indicating that there was no longer a gas connection between the surge and sump tanks and that liquid salt had entered the loop return line to the sump tank (and the discharge line from the pump volute). Slightly before 9 h on the plot, a gas breakthrough occurred in the transfer line as the salt level in the storage tank reached the bottom of the dip tube and the sump tank pressure increased sharply. With gas bubbling through the salt in the sump tank, the difference between the sump tank pressure and the storage tank pressure should correspond to the approximate salt level in the sump tank. As the storage tank pressure set point was increased further, gas bubbled through the sump tank to increase pressure in the sump tank gas head space, and the salt level in the loop continued to increase. This was eventually reflected on the surge tank level probe. There was a fair amount of variability in the sump tank pressure following the gas breakthrough. This was probably a result of chugging in the transfer line as the dip tube was covered and uncovered in the storage tank. This process eventually smoothed out after the pump was turned on and speed was increased. The reason for

this was not completely clear, although it was possible that trapped gas in the system was contributing to the pressure variations and was swept out of the flow lines as the pump speed increased.

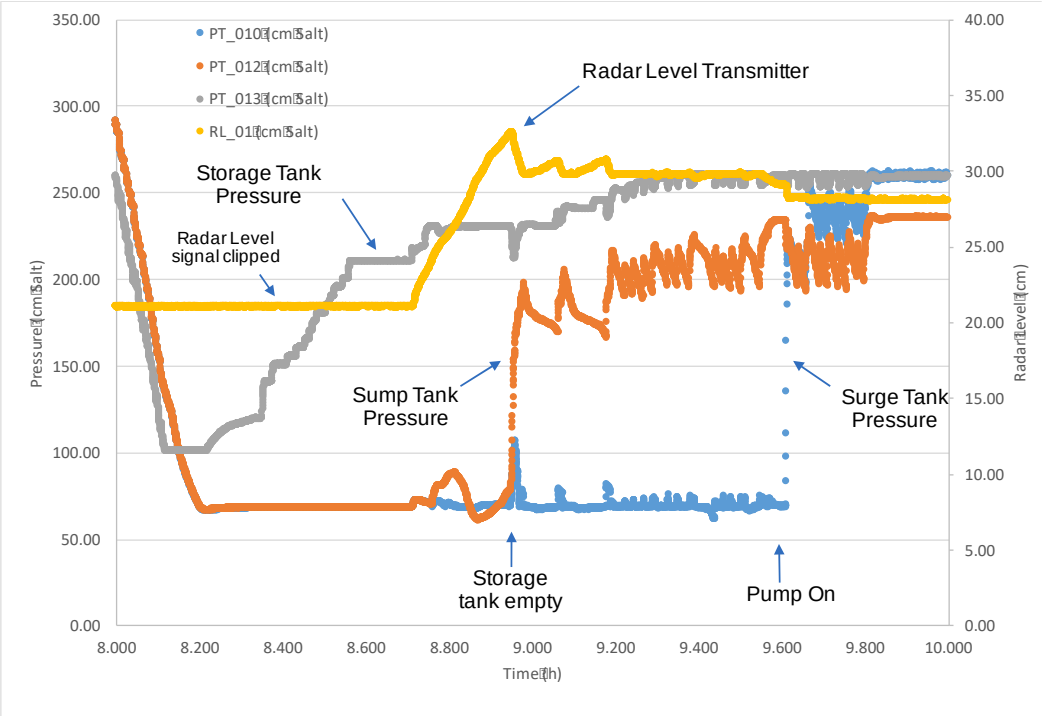

Figure 21. Example of loop fill and pump operation. The surge tank pressure (PT_010, blue) is hidden by the orange sump tank pressure (PT_012).

The radar level transmitter measurement for the sump tank is also shown in Figure 21. Because of a set-up error, the signal was cut off below ~21 cm (up to ~8.8 h on the plot).

Once the loop was full of salt, as determined by level measurement in the surge tank, and before starting the pump, the surge tank supply and vent lines were isolated. This created a closed gas volume in the top of the surge tank that was compressed when the pump started. The pump was started at 9.6 h, as indicated by the increase in surge tank pressure shown in Figure 21. Pump speed was increased twice, as shown by corresponding increases in surge tank pressure. The pump was operated at temperature for several hours to allow the circulating salt to clean the wetted loop components.

The induction power supply was turned on at a low level to verify its functionality and coupling with the pebbles. As expected, temperature ramps were observed in the instrumented pebbles on initiation of power. For this phase of loop startup, the ducts connecting the air blower to the heat exchanger were not connected, so the power that could be applied to the pebbles was limited. Consequently, these tests were of short time duration.

On closer examination of the temperature response of pebble thermocouples, a step change was observed on application of power that appeared to be noise rather than an actual pebble temperature increase. This was later confirmed and remedied during some dry tests without salt in the system and with the addition of a capacitor across the thermocouple inputs on the thermocouple module.

During a portion of testing, when the pump speed was incrementally increased, a sudden drop occurred in the indicated surge tank pressure. As the pump speed increased, the surge tank pressure also increased,

and the level in the surge tank also increased because the surge tank gas lines were isolated during testing. After investigation, it was determined that the 6.4 mm line where the pressure transducer was connected had clogged with frozen salt. It appeared that the line had a small gas leak. It is possible that the surge tank was filled completely with salt as a result of the level increasing with the pump speed, causing the salt to freeze when it reached the cold portion of the pressure transducer line, or the leak may have allowed salt vapor to condense in the cold region of the line, causing it to plug.

Once the pressure drop was noted, the salt was moved into the pump sump tank and then transferred from the pump sump tank to the storage tank. To continue shakedown operations, the surge tank pressure transducer was moved to another line, and the salt plug line was capped.

After shakedown testing was complete, the plugged line was wrapped with heating tape and insulation, and the loop pressure was reduced to just slightly over atmospheric. A Swagelok tee fitting was connected where the pressure transducer had been previously, above the salt blockage. A gas line was connected above the plugged region using the tee fitting to prevent melted salt from being pushed further up the tube and freezing again at a different location. The tube was then heated to >700°C. The gas line was pressurized with the hope the salt blockage would melt and the gas pressure would clear the line. However, the salt blockage did not melt, and the line did not clear. Therefore, while gas pressure was maintained, a stainless steel rod was pushed through the tube via the tee fitting, thus clearing the blockage.

5.3 PUMP OPERATION

The pump housing is mounted to the sump tank, and the motor is mounted to the frame (Figure 3). To accommodate differential thermal expansion between the tank and pump housing and the motor, a Lovejoy flexible drive shaft was included in the design. The Lovejoy coupling includes mounting flange faces at the top and bottom of the coupling. During initial pump startup, which occurred at room temperature and without salt, the pump experienced substantial vibration. The major cause for the excessive vibration was diagnosed as misalignment of the flexible coupling. The coupling design did not include a feature for inherent alignment of the flanged connections during assembly. The “slop” from the clearance between the bolt holes and the bolts resulted in misalignment upon assembly. Vibration was greatly reduced after careful alignment of the coupling during reassembly.

The pump was operated between 32%–59% of rated speed for a total of 16.6 h, including eight start-stop cycles. Salt temperatures in the sump ranged from 575°C –639°C. The lower speed was limited by the minimum speed required for the seal at 1,200 rpm. The highest speed was limited by the pressure of the surge tank, for which the pressure relief was set to 97 kPa (14 psig). In general, the pump performed quite well.

Over the range of conditions tested, the pump ran with only minor vibration. Before operation, accelerometers were installed on the pump housing and motor. Preliminary data were taken at 14 different pump speeds. At the flange where the shaft seal is mounted, a maximum root mean square (RMS) vibration of 0.74 m/s^2 at 58.8% speed was measured. At the top of the pump housing, the maximum RMS vibration of 1.72 m/s^2 was measured at 40.3%. This speed aligns with a natural frequency identified during vibration analysis testing[56] before operation under cold and static conditions.

Gas flow to the John Crane seal was less than 0.5 slpm, which was much less than anticipated. For most of the pump operations, the flow rate was below the range of the rotameter (2.5 slpm full scale).

Temperature measurements outside the pump housing were taken using a handheld thermocouple and an infrared camera. The temperature near the seal was approximately 52°C. This is about the same as the

temperature measured during shakedown testing at room temperature without salt. The temperature of the housing right above the sump tank insulation was approximately 151°C.

5.4 INSTRUMENTATION PERFORMANCE

The system employs a FLEXIM ultrasonic flowmeter on the molten salt return line to the sump tank. Waveguides and associated hardware are attached to the outside of the 25 mm (1 in.) pipe (Figure 7and Figure 18). As noted, the flowmeter was not operational during this initial start-up. Extensive testing of the flowmeter was performed on a water loop that allowed familiarization with the instrument and experience in setting up waveguide spacing and other settings. In addition, a separate flow calibration facility is being constructed to perform evaluation and calibration of the meter with molten salt at representative temperatures.

A high-temperature pressure transmitter manufactured by GP:50 was installed on the discharge of the pump, inside the sump tank. Pressure is transmitted through a diaphragm at the molten salt interface through a NaK-filled capillary channel contained in an Inconel 600 extension rod to a transmitter on the cooler end. During a calibration check of the instrument during shakedown of the loop, it was discovered that the NaK had leaked out through a crack in the diaphragm. The instrument had been installed in the sump tank for a couple years and had only been exposed to conditioned air—not molten salt—when it failed. Residue from the NaK was found in the discharge pipe below the location of the diaphragm. A replacement had not been received at the time of this test phase.

A Vega radar level transmitter is installed on the sump tank. The transmitter appeared to work when measuring the salt level (Figure 21), although the transmitter was not set up correctly before this test operation. The 4–20 mA output signal was cut off at salt levels of ~21 cm and did not show values below this level. However, even with the set-up problem, the radar-based level detector worked well at indicating relative level changes in the sump tank. It provided a continuous level indication and responded much faster than the heated thermocouple-based level detectors that were installed in all of the tanks.

Heated thermocouple-type level probes manufactured by Delta M are installed in all three of the vessels. The probes consist of a center heater cable and an array of thermocouples spaced axially along the length of the probe, all swaged inside a nickel outer sheath with an outer diameter of 6.35 mm (0.25 in.). A pair of probes is used to make the level measurement. One of the probes was heated, and the other was left unheated. Comparison of thermocouples on the heated and unheated probes at the same axial level will indicate when they are in a gas region or a liquid region. To set up the heated probe, current from a power supply operated in constant current control mode was adjusted to produce a temperature rise of 15–20°C (for the gas condition). Heat transfer in the liquid region is much higher, and the low power applied to the probe is not sufficient under this condition to raise the temperature of the thermocouple significantly compared to the unheated probe. These probes appeared to work well, although the response was somewhat slow and may have been affected by transient wetting of the probes above the actual salt level. The probes are also limited to taking measurements at the discrete thermocouple locations.

5.5 PIPING AND FITTINGS

Swagelok compression fittings are used in several locations on the loop and clean-up systems. They were included for all of the gas lines except for those that contained HF or H_2 outside the hood (these were welded). All of the loop tanks and the purification system crucible had tubing welded into the tank flanges that extended above the insulation, thus allowing the compression fittings to remain at relatively low temperature during operation (see top flange in Figure 9). Unlike the gas lines that were directly connected to the extension tubes, the salt transfer tubes ran to the bottom of each tank through one of the tube extensions. The transfer tubing was connected to the extension using a bored-through compression

fitting. This functioned as a gas seal because the salt flowed through the transfer tube and not the extension tube. Because the transfer tubing temperature had to be maintained above the salt's melting temperature (target temperatures were typically 550°C or above), the compression fittings operated at high temperatures. These fittings were sometimes difficult to loosen, in some instances requiring that the tubing be cut to effect removal. Both the threaded portion of the fitting and the tube-to-fitting connection seized at some locations. It was found that using a bored-through Swagelok reducer with a Swagelok union worked better than a bored-through Swagelok reducing union because the fitting could be broken loose at the larger diameter reducer-to-union fitting to avoid pulling the tube through the close tolerance of the bored-through section. This set-up also provides another option if the first choice proves to be too difficult to loosen.

6. CONCLUSION

The LSTL, a high-temperature liquid fluoride salt forced convection test facility, has been assembled, and shakedown testing has been performed at ORNL. With the successful startup in 2016, this is the first time in approximately 40 years that this type of facility has been operated in the United States. The facility incorporates a significant number of new technologies not previously tested for salt use. A significant amount of practical experience was developed during the course of starting up this loop, and the descriptions provided here should help those trying to develop similar technologies. The results of this testing effort have showed that the facility worked very well, but several areas for improvement were identified to enhance future testing.

REFERENCES

1. Brian, R.C., Weinberg, A.M., 1957. "Molten Fluorides as Power Reactor Fuels," *Nuclear Science and Engineering* 2(6), 797–803.
2. Bettis, E.S., et al., 1957. "The Aircraft Reactor Experiment—Design and Construction," *Nuclear Science and Engineering* 2(6), 804–825.
3. Ergen, W.K., et al., 1957. "The Aircraft Reactor Experiment—Physics," *Nuclear Science and Engineering* 2(6), 826–840.
4. Bettis, E.S., et al., 1957. :The Aircraft Reactor Experiment—Operation," *Nuclear Science and Engineering* 2(6), 841–853.
5. Haubenreich, P.N., Engel, J.R. 1970. "Experience with the Molten-Salt Reactor Experiment," *Nuclear Applications and Technology* 8, 118–136.
6. Bettis, E.S., Alexander, L.G., Watts, H.L. 1972. *Design Studies of a Molten-Salt Reactor Demonstration Plant*, ORNL-TM-3832, Oak Ridge National Laboratory, Oak Ridge, TN.
7. Manly, W.D., et al., 1957. *Aircraft Reactor Experiment–Metallurgical Aspects*, ORNL-2349, Oak Ridge National Laboratory, Oak Ridge, TN.
8. Cantor, S., 1973. *Density and Viscosity of Several Molten Fluoride Mixtures*, ORNL-TM-4308, Oak Ridge National Laboratory, Oak Ridge, TN.
9. Cantor, S., et al., 1968. *Physical Properties of Molten-Salt Reactor Fuel, Coolant, and Flush Salts*, ORNL-TM-2316, Oak Ridge National Laboratory, Oak Ridge, TN.
10. Powers, W.D., Cohen, S.I., Greene, N.D. 1963. "Physical Properties of Molten Reactor Fuels and Coolants," *Nuclear Science and Engineering* 17(2), 200–211.
11. Silverman, M.D., Huntley, W.R., Robertson, H.E., 1976. *Heat Transfer Measurements in a Forced Convection Loop with Two Molten-Fluoride Salts: LiF-BeF_2-ThF_2-UF_4 and Eutectic $NaBF_4$-NaF*, ORNL/TM-5335, Oak Ridge National Laboratory, Oak Ridge, TN.
12. Carlsmith, R.S., 1967. *Review of Molten Salt Reactor Physics Calculations*, ORNL-TM-1946, Oak Ridge National Laboratory, Oak Ridge, TN.
13. Guymon, R.H. (Ed.), 1973. *MSRE Systems and Components Performance*, ORNL-TM-3039, Oak Ridge National Laboratory, Oak Ridge, TN.
14. Shaffer, J.H. 1971. *Preparation and Handling of Salt Mixtures for the Molten Salt Reactor Experiment*, ORNL-4616, Oak Ridge National Laboratory, Oak Ridge, TN.
15. Thomas, R.E. (Ed.), 1959. *Phase Diagrams of Nuclear Reactor Materials*, ORNL-2548, Oak Ridge National Laboratory, Oak Ridge, TN.
16. Hogland, B., "Fluid fluorides and chlorides reactor research and development on molten salt reactors (MSRs) papers, books, and reports." https://moltensalt.org/references/static/downloads/pdf/, accessed July 3, 2023.
17. Generation IV International Forum. http://www.gen-4.org/.
18. US DOE Nuclear Energy Research Advisory Committee and the Generation IV International Forum, 2002. *A Technology Roadmap for Generation IV Nuclear Energy Systems*, GIF-002-00.
19. Forsberg, C.W., Peterson, P.F., Pickard, P.S., 2003. "Molten-Salt-Cooled Advanced High-Temperature Reactor for Production of Hydrogen and Electricity," *Nuclear Technology* 144, 289–302.
20. Merle-Lucotte, E., et al., 2011. "Launching the Thorium Fuel Cycle with the Molten Salt Fast Reactor," *Proceedings of the International Congress on Advances in Nuclear Power Plants*, Nice, France.
21. Renault, C. et al., 2009. "The Molten Salt Reactor (MSR) in Generation IV: Overview and Perspectives," GIV Symposium, Paris, France, September 9–10, 191–200.
22. Luo, Y., Gaspar, M. 2016. "Molten Salt Reactors: IAEA to Establish a New Platform for Collaboration." International Atomic Energy Agency. https://www.iaea.org/newscenter/news/molten-salt-reactors-iaea-to-establish-new-platform-for-collaboration

23. Ingersoll, D., et al., 2004, *Status of Pre-Conceptual Design of the Advanced High-Temperature Reactor (AHTR)*, ORNL/TM-2004/104, Oak Ridge National Laboratory, Oak Ridge, TN.
24. Varma, V., et al., 2012. *AHTR Mechanical, Structural, and Neutronic Preconceptual Design*, ORNL/TM-2012/320, Oak Ridge National Laboratory, Oak Ridge, TN.
25. Greene, S.R., 2010. "SmAHTR–A Concept for a Small Advanced High Temperature Reactor," *Proceedings of HTR-10*, Prague, Czech Republic.
26. Bardet, P., et al., 2009. "Design, Analysis, and Development of the Modular PBAHTR," *Proceedings of the International Congress on Advances in Nuclear Power Plants*, Tokyo, Japan, May 10–14, 161–178.
27. Scarlat, Raluca O., et al. "Design and licensing strategies for the fluoride-salt-cooled, high-temperature reactor (FHR) technology." *Progress in Nuclear Energy* 77 (2014): 406-420.
28. Zhang, Dingkang, and Rahnema, Farzad. Integrated Approach to Fluoride High Temperature Reactor Technology and Licensing Challenges (FHR-IRP). United States: N. p., 2019. Web. doi:10.2172/1505504.
29. Yu, X., Xu, H., 2016. "Update on SINAP TMSR Research." Presented at the MSR Workshop, Oak Ridge National Lab, Oak Ridge, TN, October 4–5.
30. Safety Assessment of the Molten Salt Fast Reactor. http://samofar.eu/, accessed July 5, 2023.
31. Hron, M.,Kyncl, J., Mikisek, M., 2009. "Reactor Physical Experimental Program EROS in the Frame of the Molten Salt Applying Reactor Concepts Development." *Proceedings of the International Congress on Advances in Nuclear Power Plants*, Tokyo, Japan, May 10–14.
32. Singh, I. et al., "Preliminary Physics Design of Pebble Bed HTR with FLiBe Coolant," Technical Meeting on the Status of Deep-Burn Concepts for High Temperature Gas Cooled Reactors, December 7–9, 2015.
33. Novikov, V.M. 1995. "The Results of the Investigations of Russian Research Center 'Kurchatov Institute' on Molten Salt Applications to Problems of Nuclear Energy Systems," International Conference on Accelerator-Driven Transmutation Technologies and Applications, 346, 138–147.
34. Serp, J., et al., 2014. "The Molten Salt Reactor in Generation IV: Overview and Perspectives." *Progress in Nuclear Energy* 77, 308–319. http://dx.doi.org/10.1016/j.pnucene.2014.02.014
35. Gilleland, J. 2016. "Terra Power's Continuing Innovation." http://terrapower.com/news/terrapowers-continuing-innovation. Accessed July 5, 2023.
36. "Terrestrial Energy." https://www.terrestrialenergy.com/. Accessed July 5, 2023.
37. "Flibe Energy." http://flibe-energy.com/. Accessed July 5, 2023.
38. Transatomic Power. http://transatomicpower.com/. Accessed July 5, 2023.
39. Elysium Industries. https://www.forbes.com/sites/llewellynking/2020/10/13/new-design-molten-salt-reactor-is-cheaper-to-run-consumes-nuclear-waste. Accessed July 5, 2023.
40. Devanney, J., 2012. *ThorCon Summary Description*. Version 0.60, Martingale Inc., Sisyphus Beach, Tavernier, FL.
41. Robinson, B.K., "Advanced Reactor Concepts 2015 (ARC 15)," DOE-NRC 2016 Advanced Reactor Workshop, June 7, 2016. NRC Accession No. ML16155A242.
42. US Department of Energy. 2016. "Department of Energy Fostering Public-Private Partnerships: Eight Small Businesses Selected for First GAIN Nuclear Energy Vouchers." http://energy.gov/ne/articles/department-energy-fostering-public-private-partnerships-eight-small-businesses-selected. Accessed July 5, 2023.
43. Grimes, W.R., Cantor, S., 1972. *Molten Salts as Blanket Fluids in Controlled Fusion Reactors*, ORNL-TM-4047, Oak Ridge National Laboratory, Oak Ridge, TN.
44. Saltmarsh, M.J., 1979, *Optimization of the Fission-Fusion Hybrid Concept*, ORNL/PPA-79/3, Oak Ridge National Laboratory, Oak Ridge, TN.
45. Abdou, M., et al., 2005. "U.S. Plans and Strategy for ITER Blanket Testing," *Fusion Science and Technology* 47, 475–487.
46. Sze, D.K., et al., 1986. "Conceptual Design of a Self-Cooled FLiBe Blanket," *Fusion Technology* 10(3), 624–632.

47. Abdou, M.A., et al., 2005. “Overview of Fusion Blanket R&D in the US over the Last Decade,” *Nuclear Engineering and Technology* 37(5), 401–422.
48. Moir, R.W., et al., 1985. “Helium-Cooled, FliBe Breeder, Beryllium Multiplier Blanket,” *Fusion Technology* 8(1), Part 1, 133–148.
49. Moir, R.W., Lee, J.D. 1986. “Helium-Cooled, FLiBe-Breeder, Beryllium-Multiplier Blanket for MINIMARS,” *Fusion Technology* 10(3), Part 2(A), 619–623.
50. Misra, A.K., Whittenberger, J.D. 1987. “Fluoride Salts and Container Materials for Thermal Energy Storage Applications in the Temperature Range 973–1400 K,” *Proceedings of Energy-New Frontiers, American Institute of Aeronautics and Astronautics*, Philadelphia, PA, (AIAA-87-9226) 188–201.
51. Yoder, G.L., Aaron, A., Cunningham, B., Fugate, D., Holcomb, D., Kisner, R., Peretz, F., Robb, K., Wilgen, J., Wilson, D., 2014. “An Experimental Test Facility to Support Development of the Fluoride-Salt-Cooled High-Temperature Reactor,” *Annals of Nuclear Energy* 64, 511–517.
52. Yoder, G.L., Aaron, A., Cunningham, R.B., Fugate, D., Holcomb, D., Kisner, R. Peretz, F., Robb, K., Wilson, D., 2012. *High-Temperature Fluoride Salt Test Loop*, ORNL/TM-2012.
53. Yoder, G.L., Aaron, A., Heatherly, D., Holcomb, D., Kisner, R. McCarthy, M, Peretz, F., Wilgen, J., Wilson, D., 2011. “An Experiment to Study Pebble Bed Liquid-Fluoride-Salt Heat Transfer,” *Proceedings of the International Congress on Advances in Nuclear Power Plants*, Nice, France, May 2–5.
54. Yoder, G.L., Aaron, A., Heatherly, D. Holcomb, D., Kisner, Peretz, F., Romanoski, G. Wilgen, J., Wilson, D., 2010. Development of a Forced-Convection Liquid Salt Test Loop,” *Proceedings of HTR 10*, Prague, Czech Republic, October 18–20.
55. Tunnell, W. C., 1956. *Seals and Packing Materials for Molten Fluoride Salts*, ORNL-TM-386, Oak Ridge National Laboratory.
56. Robb, K.R., Jain, P.K., Hazelwood, T.J., 2016. *High-Temperature Salt Pump Review and Guidelines—Phase I Report*, ORNL/TM-2016/199, Oak Ridge National Laboratory, Oak Ridge, TN.